Dynamics of Solvent and Rotational Relaxation of Glycerol in the Nanocavity of Reverse Micelles

Anjan Chakraborty, Debabrata Seth, Palash Setua, and Nilmoni Sarkar*

Department of Chemistry, Indian Institute of Technology, Kharagpur 721 302, WB, India

Received: November 17, 2005; In Final Form: January 25, 2006

The dynamics of solvent and rotational relaxation of Coumarin 480 and Coumarin 490 in glycerol containing bis-2-ethyl hexyl sulfosuccinate sodium salt (AOT) reverse micelles have been investigated with steady-state and time-resolved fluorescence spectroscopy. We observed slower solvent relaxation of glycerol confined in the nanocavity of AOT reverse micelles compared to that in pure glycerol. However, the slowing down in the solvation time on going from neat glycerol to glycerol confined reverse micelles is not comparable to that on going from pure water or acetonitrile to water or acetonitrile confined AOT reverse micellar aggregates. While solvent relaxation times were found to decrease with increasing glycerol content in the reverse micellar pool, rotational relaxation times were found to increase with increase in glycerol content.

1. Introduction

Reverse micelles are one of the interesting models for biomembranes among the different organized assemblies.[1−3] They are an important reactor for heterogeneous chemistry and templates for nanostructure and are often used as a vehicle for drug delivery.[4,5] In general surfactant molecules undergo self-aggregation with their polar headgroups on the interior and solubilize a small amount of polar solvents such as water, methanol, acetonitrile, etc., creating a new confined liquid phase on the inside.[1−8] The most common surfactant used to create reverse micelles is Aeorosol-OT (AOT), and water is often used as the polar solvent. The solvent pool is defined over a wide range of solvent and surfactant concentration by a single parameter,

$$w_s = [H_2O]/[AOT]$$

This confinement makes the polar solvent different in behavior from pure solution. Thus, studies of many interesting photophysical works, charge transfer, energy transfer, exciplex formation, etc. have been carried out in reverse micelles.[9]

One of the most useful methods often used to investigate the dynamics of polar solvent is the time dependent fluorescence Stokes' shift of a solvatochromic probe molecule popularly known as solvation dynamics. Thus there are several reports regarding the solvation dynamics starting from convetional polar solvents[10−19] such as water, methanol, and acetonitrile to different organized media such as micelles,[20−23] mixed micelles,[24] star-like macromolecules,[25] lipids,[26] proteins,[27,28] aqueous and nonaqueous reverse micelles, etc.[29−42] Since we are concerned with only reverse micellar systems in the present study, let us summarize the striking observations of solvent relaxation in the solvent pool of reverse micelles.

Sarkar et al.[29] and Das et al.[30] investigated solvation dynamics in aqueous AOT reverse micelles using picosecond laser spectroscopy and found that solvent relaxation is many times slower in the water pool of the reverse micelles compared to that in pure solution. Levinger et al.[31−36] investigated solvation dynamics in various reverse micelles using femtosecond fluorescence upconversion spectroscopy. They[33] examined the effect of counterion on the solvation dynamics. It was that found that when Na^+ is replaced by NH_4^+ ions in AOT surfactant, the solvation dynamics becomes faster. It is reported that water motion is essentially frozen inside the reverse micellar core at low water content while at higher water content the reverse micellar pool becomes larger and an additional bulk-type relaxation is observed.[33]

Although in the literature numerous studies are available regarding solvation dynamics in aqueous reverse micelles,[20−22,29−38] there are few reports regarding the solvation dynamics in nonaqueous reverse micelles using polar solvents other than water.[39−42] Recently Levinger et al. characterized the various types of reverse micelles in AOT using formamide, ethylene glycol, actonitrile, methanol, *N*,*N*-dimethylformamide, 1,2-propanediol, etc. as cosolvents.[8] They reported solvation dynamics in formamide/AOT/isooctane reverse micelles.[39] It was observed that formamide is immobilized in the reverse micellar pool. Shirota et al.[40] reported solvation dynamics in reverse micelles using methanol and acetonitrile as the polar solvent pool. Recently we reported solvation dynamics in methanol and acetonitrile reverse micelles.[41] It is observed by Shirota et al.[40] and by our group[41] that solvation dynamics inside the reverse micellar pool is highly dependent on the hydrogen bonding network. With increasing methanol content, the solvation dynamics becomes faster while it is insensitive to the change in acetonitrile content. This phenomenon was explained by dynamic exchange model by Shirota et al.[40] and us.[41] Shirota et al.[42] very recently studied solvation dynamics in formamide/AOT/isooctane and *N*,*N*-dimethylformamide/AOT/isooctane reverse micelles. In both cases they observed that with increasing solvent content the solvation dynamics becomes faster. However, the change in solvation time is more sensitive for formamide than that for *N*,*N*-dimethylformamide. The fact is attributed to the higher tendency of formamide to form hydrogen bonds with the polar headgroup of AOT surfactant molecules than that of *N*,*N*-dimethylformamide. Besides the experimental studies of solvent relaxation in confined cavities[20−22,29−42] of water and

* Address correspondence to this author. E-mail: nilmoni@chem.iitkgp.ernet.in. Fax: 91-3222-255303.

10.1021/jp056650c CCC: $33.50 © 2006 American Chemical Society
Published on Web 02/25/2006

CHART 1

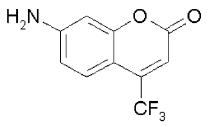

Coumarin 490 (C-490)

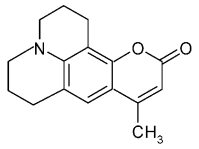

Coumarin 480 (C-480)

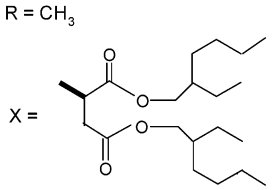

Dioctylsulphosuccinate, sodium salt (AOT)

other polar cosolvents, there are also several simulation studies[43−47] to unravel the dynamical features in confined assemblies. All these simulation studies suggested the existence of biexponential solvent relaxation in the confined cavity. Recently vibration relaxation dynamics of azide ions in ionic and nonionic reverse micelles were investigated by Owrutsky et al.[48] Kelkar et al.[49] investigated depth-dependent solvent relaxation in reverse micelles using steady-state and time-resolved fluorescence spectroscopy.

In this paper we report solvent and rotational relaxation in pure glycerol and glycerol containing reverse micelles. The main reasons behind choosing glycerol reverse micelles for solvent relaxation studies are 3-fold. First glycerol has a much higher viscosity than most of conventional solvents. The solvent relaxation in this solvent[16] is quite slow and this can be detected in the picosecond setup. Previously we could not report solvation dynamics of pure solvent used for AOT reverse micelles due to limited time resolution of our setup. Second, glycerol has an extensive hydrogen-bonding network; often it forms hydrogen bonds to solute molecules. Third, in recent years there have been many solvent relaxation studies[50−52] in environment friendly room-temperature ionic liquids (ILs). Thus ionic liquids confined in the nanocavity became interesting systems in which to study the solvent relaxation process in a nanometer size cavity.[53−55] Since ionic liquids have a very high viscosity compared to that of isopolar solvent, it would be interesting to investigate solvent relaxation in a very high viscous solvent compared to IL within a confined cavity.

In this work we have used two probes, namely Coumarin 490 and Coumarin 480 (shown in Chart 1), to monitor the dynamical Stokes' shift. The rotational relaxation studies have also been performed. The results have been analyzed with the existing theories and other experimental observations. To the best of our knowledge this the first report of the solvation dynamics in glycerol reverse micelles.

2. Experimental Section

C-490 and C-480 (laser grade from Exciton) were used as received. AOT (dioctylsulfosuccinate, sodium salt, Aldrich) was purified by standard procedure.[41] Isooctane, spectroscopic grade (Spectrochem), was freshly distilled over calcium hydride (Spectrochem) before use. Glycerol was purchased from Aldrich and was used as received. Glycerol content inside the reverse micellar pool is defined as w_g = [glycerol]/[AOT].

TABLE 1: Steady-State Absorption and Emission Maxima of C-480 and C-490 in Isooctane/AOT/Glycerol at Different w_g Values

	C-480		C-490	
system	λ_{abs}(max)/nm	λ_{em}(max)/nm	λ_{abs}(max)/nm	λ_{em}(max)/nm
isootcane	363	406	347	400
glycerol	400	482	379	492
isooctane/AOT/glycerol				
$w_g = 0$	363	445	379	440
$w_g = 1.9$	363	463	379	472
$w_g = 3$	363	466	379	476
$w_g = 3.7$	363	468	379	478

The concentration of probe molecules maintained in all the measurements is 4×10^{-5} M and that of AOT is 0.09 M. The preparation of glycerol reverse micelles was done according to the procedure described by Costa et al. in recent publications.[56]

For absorption and fluorescence measurements we used a Shimadzu absorption spectrophotometer (model no. UV 1601) and a Spex-fluorolog-2 spectrofluorimeter, respectively. The fluorescence spectra were corrected for wavelength sensitivity of the detection system and were obtained as a photon number intensity spectrum. The experimental setup for picosecond time correlated single photon counting (TCSPC) was as follows. Briefly, a picosecond diode laser at 408 nm (IBH, UK, NanoLED-07) is used as a light source. The fluorescence signal was detected in magic angle (54.7°) polarization using Hamamatsu MCP PMT (3809U). The typical system response of this laser system is ~90 ps. The decays were analyzed with IBH DAS-6 decay analysis software. The same setup was used for anisotropy measurements. For the anisotropy decays, we used a motorized polarizer in the emission side. The emission intensities at parallel ($I_{||}$) and perpendicular ($I_{\perp}$) polarizations were collected alternatively until a certain peak difference between parallel ($I_{||}$) and perpendicular ($I_{\perp}$) decay was reached. The peak differences depended on the tail matching of the parallel ($I_{||}$) and perpendicular ($I_{\perp}$) decays. The analysis of the data was done with IBH DAS 6 decay analysis software. The same software was also used to analyze the anisotropy data.

The temperature was kept 298 ± 1 K for all measurements.

3. Results and Discussions

3.1. Steady-State Absorption and Emission Spectra. The absorption and emission spectra were taken in isooctane and in glycerol reverse micelles. The absorption and emission maxima are listed in Table 1. In pure isooctane solution the absorption maxima of C-490 and C-480 are 347 and 363 nm, respectively. In pure glycerol the absorption maxima of C-490 and C-480 are 379 and 400 nm, respectively. The absorption spectrum of C-490 in isooctane solution (347 nm) is found to be red shifted when AOT is added (379 nm). The absorbance at the red end side further increases with addition of glycerol to C-490/isooctane/AOT solution. This is illustrated in Figure 1a. On the other hand, we did not observe such a peak shift in the absorption spectra on addition of AOT to an isooctane solution (363 nm) of C-480. However, on addition of AOT to an isooctane solution of C-480, a distinct shoulder is found to grow at the red end side. This indicates that a substantial number of C-480 molecules migrate from bulk solvent to the reverse micellar solvent pool. The absorbance spectra of C-480 are illustrated in Figure 1b.

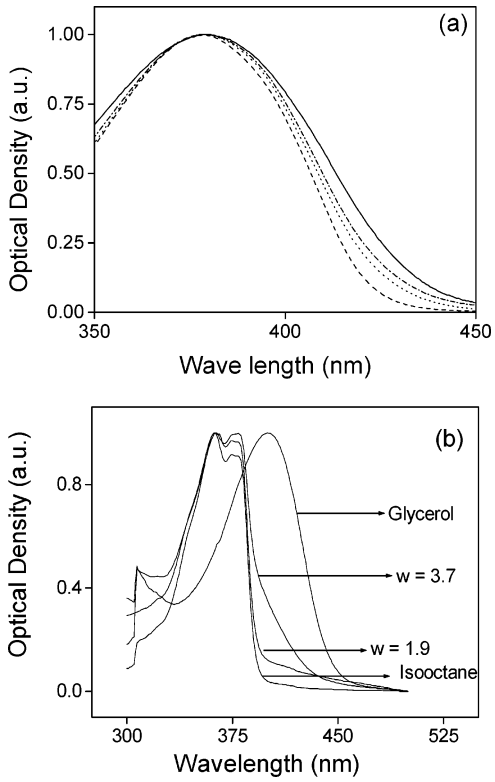

Figure 1. (a) Steady-state normalized absorption spectra of C-490 in pure glycerol, and in glycerol reverse micelles at $w_g = 0$, 1.9, and 3.7. Solid lines for pure glycerol, dash line for $w_g = 0$, dot line for $w_g = 1.9$, and dash-dot line for $w_g = 3.7$. (b) Steady-state normalized absorption spectra of C-480 in isooctane, pure glycerol, in glycerol reverse micelles at $w_g = 1.9$ and 3.7.

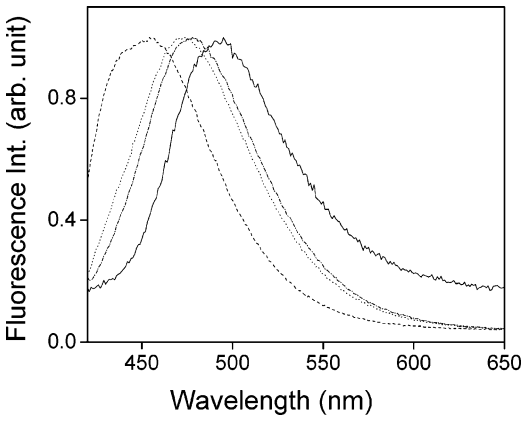

Figure 2. Steady-state normalized emission spectra of C-490 in pure glycerol, at glycerol reverse micelles at $w_g = 0$, 1.9, and 3.7. Solid lines for pure glycerol, dash lines for $w_g = 0$, dot lines for $w_g = 1.9$, and dash-dot line for $w_g = 3.7$.

TABLE 2: Rotational Relaxation Time (τ_r) of C-490 and C-480 in Isooctane/AOT/Glycerol at Different w_g Values

(a) C-490

system	w_g	r_0	a_{1r}	τ_{1r} (ns)	a_{2r}	τ_{2r} (ns)	$\langle\tau_r\rangle^a$
isooctane/AOT	0	0.38	0.55	0.66	0.45	1.85	1.20
isooctane/AOT/glycerol	1.9	0.35	0.20	0.38	0.80	6.18	5.0
isooctane/AOT/glycerol	3	0.33	0.18	0.79	0.82	9.47	7.90
isooctane/AOT/glycerol	3.7	0.36	0.20	1.0	0.80	10.55	8.64

(b) C-480

system	w_g	r_0	a_{1r}	τ_{1r} (ns)	a_{2r}	τ_{2r} (ns)	$\langle\tau_r\rangle^a$
isooctane/AOT	0	0.38	0.38	0.68	0.62	1.80	1.37
isooctane/AOT/glycerol	1.9	0.35	0.15	0.76	0.85	6.86	5.94
isooctane/AOT/glycerol	3	0.35	0.15	0.950	0.85	9.94	8.6
isooctane/AOT/glycerol	3.7	0.36	0.19	1.0	0.81	10.55	8.73

[a] Error in the measurement is ±5%.

It is revealed from Figure 1b that absorption at the red end side further increases with addition of glycerol to the C-480/isooctane/AOT solution.

In pure glycerol the emission maxima of C-490 and C-480 are 492 and 482 nm, respectively. In pure isooctane the emission peaks of C-490 and C-480 are 400 and 406 nm, respectively. After addition of AOT to Coumarin/isooctane solution the emission maxima of C-490 and C-480 become 440 and 445 nm, respectively. The spectra are further red shifted when glycerol is added to Coumarin/isooctane/AOT systems and at $w_g = 3.7$ glycerol content the observed emission peaks are 478 and 468 nm for C-490 and C-480, respectively. The fact implies that both the probes experience a more polar environment in the solvent pool of the reverse micelles. The representative emission spectra of C-490 in pure glycerol and in glycerol reverse micelles at different w_g values are shown in Figure 2. The emission peaks of C-490 and C-480 in pure isooctane, in glycerol, and in AOT reverse micelles at different w_g values are listed in Table 1.

3.2. Time-Resolved Anisotropy Measurements. Absorption and emission spectra can give a qualitative idea regarding the location of the probe molecules. This can be more accurately predicted by the time-resolved fluorescence anisotropy. Time-resolved fluorescence anisotropy $r(t)$ is calculated with the following equation

$$r(t) = \frac{I_{||}(t) - GI_{\perp}(t)}{I_{||}(t) + 2GI_{\perp}(t)} \quad (1)$$

where G is the correction factor for detector sensitivity to the polarization direction of the emission. In our case the value of G is 0.6. $I_{||}(t)$ and $I_{\perp}(t)$ are fluorescence decays polarized parallel and perpendicular to the polarization of the excitation light, respectively. The anisotropy decay parameters are listed in Table 2. Representative anisotropy decays of C-490 and C-480 micelles at $w_g = 3$ and 3.7 are shown in Figure 3. The anisotropy decays in reverse micelles are found to be bimodal in nature. We[57] previously reported that Coumarin molecules C-152, C-481, and C-153 have rotational time around 100 ps in pure *n*-heptane. As the emission maxima of C-490 and C-480 in pure isooctane are almost close to the excitation wavelength (~408 nm), we cannot report the rotational relaxation time of these dyes in pure isooctane. Table 2 reveals that rotational relaxation times of C-490 and C-480 are much longer in reverse micelles compared to that in pure solvents such as pure water and *n*-heptane. Moreover, the anisotropy decays of the probe molecules in the presence and absence of glycerol molecules are vastly different. The rotational relaxation times of C-490 and C-480 at $w_g = 0$, i.e., without addition of glycerol, are 1.2 and 1.37 ns, respectively. With addition of glycerol the rotational time increases and at $w_g = 3.7$ the rotational relaxations times for C-490 and C-480 become 8.64 and 8.73 ns. The high rotational relaxation times in the presence of glycerol indicate that probe molecules experience a different environment inside the solvent pool from that in pure isooctane or in the absence of glycerol. Again it is revealed from Table 2 that with increasing the glycerol content of reverse micelles the rotational relaxation time also increases. The rotational relaxation times for C-490 and C-480 at $w_g = 1.9$ are 5.0 and 5.94 ns. At the highest glycerol content, i.e., at $w_g = 3.7$, rotational relaxation

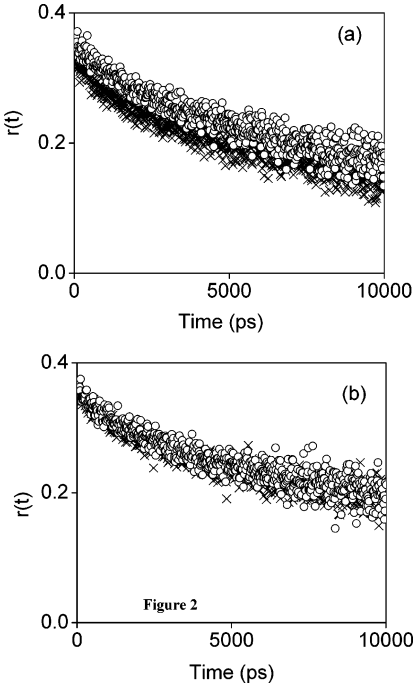

Figure 3. Decays of fluorescence anisotropy $r(t)$ of C-480 (○) and C-490 (×) at $w_g = 3.0$ (a) and 3.7 (b).

times become 8.64 and 8.73 ns. This is due to the fact that with addition of more and more glycerol, the viscosity of the medium as well as the hydrogen bonding probability of the probe molecules to the solvent increases; hence we see an increase in the average rotational relaxation time.

Glycerol has very high viscosity due to its extensive hydrogen-bonding network. One molecule of glycerol possesses three hydroxyl groups. Thus the hydrogen bonding in pure glycerol is much stronger than that in ordinary solvent. Glycerol can bind to the solute molecules. From Table 2 we observe that at low glycerol content (at $w_g = 1.9$) C-490 has faster rotational relaxation (5.0 ns) than C-480 (5.94 ns). However, with increasing glycerol content the rotational relaxation times of both probes become closer and when glycerol content is highest, i.e., at $w_g = 3.7$, they have the same rotational relaxation time (8.64 ns for C-490 and 8.73 ns for C-480). The obvious reason is that C-490 possesses an $-NH_2$ group that is attached strongly to glycerol molecules with hydrogen bonding whereas C-480 is a rigid molecule and solvent attachment for this molecule is rather weaker. Another interesting observation is that in case of C-480 at $w_g = 3$ and 3.7 the rotational relaxation times are very close (8.6 ns at $w_g = 3$ and 8.75 ns at $w_g = 3.7$, respectively) while for C-490 at $w_g = 3$ and 3.7 rotational relaxation times are quite different (7.90 ns at $w_g = 3$ and 8.65 ns at $w_g = 3.7$, respectively). This is due to the fact with increasing glycerol content inside the reverse micellar solvent pool C-490 molecules will form stronger hydrogen bonding owing to its $-NH_2$ group. Thus a steady increase form 7.9 ns (at $w_g = 3$) to 8.64 ns (at $w_g = 3.7$) is observed in the average rotational relaxation time observed. On the other hand C-480 being a rigid molecule would have less tendency to form hydrogen bonding with the glycerol molecules. Thus a little increase from 8.60 ns (at $w_g = 3$) to 8.75 ns (at $w_g = 3.7$) in average rotational relaxation time is observed. The other probability is that C-480 being hydrophobic in nature, a small amount of C-480 molecule may reside in the interface of the reverse micelles by partitioning between the interface and the solvent pool. If it were true, the molecules residing in the interface would experience a less glycerol-like environment hence they would have a less viscous environment. These molecules will exhibit faster rotational relaxation time than that of the molecules inside the glycerol solvent pool and will contribute to the average rotational relaxation. Thus we observe almost the same average rotational relaxation for C-480 at $w_g = 3$ and 3.7. In this context it would be desired to compare the rotational dynamics in glycerol to those reported previously by Costa et al.[58] These groups measured rotational dynamics and rotational friction using bis[4-(dimethylamino)phenyl]sqaraine (HSq) by fluorescence depolarization technique.[58] It was found by them that with increasing glycerol content in the reverse micelles the rotational relaxation time initially increases and becomes constant at higher glycerol content. In our case the rotational relaxation times were found to be little different at $w_g = 3$ and 3.7 for C-480, which indicates that at higher glyceol content, i.e., at $w_g = 3$ and 3.7, C-480 molecules experience the same viscosity. This observation also leads to the conclusion that most of the dye molecules reside in the solvent pool. The comparatively larger difference in rotational times at $w_g = 3$ and 3.7 for C-490 is ascribed to the hydrogen bonding between C-490 and glycerol molecules as mentioned earlier. Recently Dutt[59] and Topp[60] reported some interesting results where the effects of hydrogen boning have been briefly discussed.

TABLE 3: Analytical Rotational Parameters of C-490 and C-480 in Isooctane/AOT/Glycerol Systems

(a) C-490

w_g	τ_m (ns)	τ_e (ns)	τ_D (ns)	$10^{-8}D_w$ (S^{-1})	θ_0 (degree)	S
1.9	9.66	0.40	16.95	1.10	22.0	0.89
3	36.5	0.86	12.81	0.46	21.28	0.90
3.7	93.00	1.10	11.89	0.38	22.0	0.89

(b) C-480

w_g	τ_m (ns)	τ_e (ns)	τ_D (ns)	$10^{-8}D_w$ (S^{-1})	θ_0 (degree)	S
1.9	9.66	0.86	23.80	0.35	18.50	0.92
3	36.50	1.050	13.7	0.30	18.50	0.92
3.7	93.00	1.104	11.89	0.36	21.28	0.90

We calculated several rotational parameters using two-step and wobbling in a cone models.[61−63] The two-step model describes the fact that observed slow rotational relaxation is a convolution of the relaxation time corresponding to the overall rotation of the micelles (τ_m) and lateral diffusion of the probe (τ_D). The wobbling in a cone model describes the internal motion of the probe (τ_e) in terms of cone angle (θ_0) and wobbling diffusion coefficient (D_w). These parameters are obtained by the following equations

$$\frac{1}{\tau_2} = \frac{1}{\tau_D} + \frac{1}{\tau_m} \tag{2}$$

$$\frac{1}{\tau_1} = \frac{1}{\tau_e} + \frac{1}{\tau_2} \tag{3}$$

where τ_1 and τ_2 are the observed fast and slow components. These results are summarized in Table 3. Overall rotation of the micelles can be estimated by using the Stokes−Einstein−Debye relation

$$\tau_m = \frac{4\pi\eta r_h^3}{3kT} \tag{4}$$

where η is the viscosity of isooctane, r_h is the hydrodynamic radius of the micelles, and k and T are the Boltzmann constant and absolute temperature, respectively.

Costa et al.[56] reported the hydrodynamic radii of glycerol reverse micelles at $w_g = \sim 1.9$, ~ 3, and ~ 3.7 are 26.5, 41.5, and 56.5 Å, respectively. Thus the radii of reverse micelles are found to be increasing with increasing glycerol content. The values of τ_m are found to be increasing with the increase in glycerol content. As τ_m is of the order of several nanoseconds, it has a very negligible effect on the lateral diffusion. We have calculated the order parameters (S) from the following equation to determine the spatial restriction imposed by the solvent molecules on the probe.

$$S^2 = a_{2r} \tag{5}$$

The magnitude of S is a measure of spatial restriction and has values from 0 (unrestricted motion) to 1 (completely restricted motions).

In all cases we see that the values of S are around 0.9. The very high value of S implies that the probe molecules are facing a confined geometry. This is expected because the solvent used in the present case is of very high viscosity and hydrogen bonding ability. Thus the solvent relaxation is slower inside the reverse micellar pool. We calculated the cone angle θ_0 and wobbling diffusion coefficient as follows

$$\theta_0 = \cos^{-1}\left[\frac{1}{2}((1 + 8S)^{1/2} - 1)\right] \tag{6}$$

$$D_w = \frac{7\theta^2}{24\tau_e}D \tag{7}$$

where θ is the cone angle in radians.

The results are tabulated in Table 3. It is observed that D_w is very low in all the systems. It is also interesting to note that in most cases with an increase in glycerol content initially there is large drop in D_w, although again at higher glycerol content the D_w remains constant. This further confirms that the probe molecules are located in a confined environment in the reverse micellar core at the higher glycerol content. At the highest glycerol content (i.e., at $w_g = 3.7$) both the probes C-480 and C-490 have almost the same D_w values, which indicates that at higher glycerol content the microviscosity experienced by the probes is the same.

3.3. Dynamics of Solvent Relaxation. We studied the solvation dynamics in AOT reverse micelles at different w values by monitoring the time-resolved deacays at different wavelengths. The decays are fast at the blue end of the emission spectrum while at the red end of the emission spectrum they were preceded by a growth. The wavelength-dependent behavior of temporal decays clearly indicates that solvent relaxation is taking place in these systems. The representative decays of C-480 monitoring at three different wavelengths are shown in Figure 4. The time-resolved emission spectra (TRES) were constructed following the procedure of Fleming and Maroncelli[64] as described in our earlier publications.[41] The solvent relaxation dynamics is monitored by the solvent response function defined as

$$C(t) = \frac{\nu(t) - \nu(\infty)}{\nu(0) - \nu(\infty)} \tag{8}$$

where $\nu(0)$, $\nu(t)$, and $\nu(\infty)$ are the peak frequencies at time zero, t, and infinity, respectively. The peak frequencies were evaluated from the TRES. The representative TRES of C-490 in glycerol containing reverse micelles at $w_g = 3.7$ are shown in Figure 5. The solvent relaxation times obtained from the solvent correlation function ($C(t)$) are summarized in Table 4. The representative decays of $C(t)$ of C-490 and C-480 are shown in Figure 6. For all the systems the solvent correlation function ($C(t)$) was best fitted to a biexponential function. From Table 4 we obtained average solvation times of C-480 and C-490 in glycerol of 0.45 and 0.57 ns, respectively. In our earlier studies[41] we could not report solvation times in pure solvents used to create AOT reverse micelles because of our limited instrument response function. Glycerol is different from other polar solvents due to its extensive hydrogen-bonding network. The very high viscosity of glycerol is mainly responsible for slowing down the dynamics compared to other polar solvents. In pure water solvent relaxation occurs in the femtosecond time scale. Jimenez et al.[10] observed that solvent relaxation of C-343 in water consists of

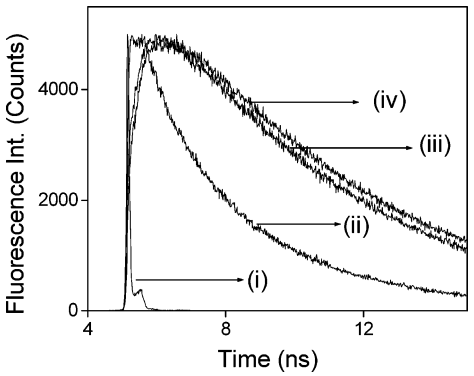

Figure 4. Fluorescence decays of C-480 in the isooctane/AOT/glycerol system at $w_g = 3.7$ (i) instrument response function (IRF), (ii) 440 nm, (iii) 530 nm, and (iv) 590 nm.

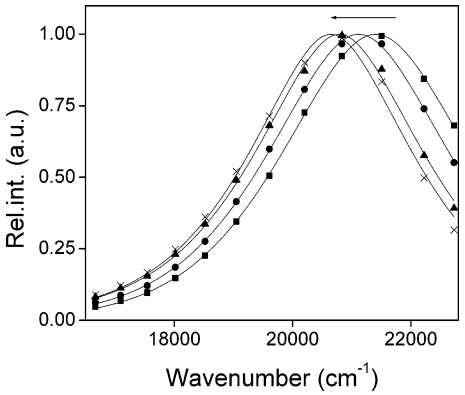

Figure 5. Time-resolved emission spectra (TRES) of C-490 in the isooctane/AOT/glycerol system at 0 (■), 1000 (●), 5000 (▲), and 10000 (×) ps.

TABLE 4: Decay Characteristics of C-490 and C-480 in Isooctane/AOT/Glycerol Systems

(a) C-490

systems	$\Delta\nu^a$ (cm^{-1})	a_1	τ_1 (ns)	a_2	τ_2 (ns)	$\langle\tau_s\rangle^b$ (ns)^c
w_g=1.9	1180	0.23	0.740	0.77	12.385	9.70
w_g=3	1095	0.30	0.883	0.70	11.320	8.20
w_g=3.7	1050	0.34	0.945	0.66	10.500	7.25
pure glycerol	1700	0.51	0.230	0.49	0.690	0.45

(b) C-480

systems	$\Delta\nu^a$ (cm^{-1})	a_1	τ_1(ns)	a_2	τ_2(ns)	$\langle\tau_s\rangle^b$ (ns)^c
w_g=1.9	2028	0.25	0.863	0.75	13.800	10.56
w_g=3	1903	0.30	0.821	0.70	11.947	8.61
w_g=3.7	1959	0.35	0.790	0.65	12.053	8.11
pure glycerol	900	0.69	0.460	0.31	0.827	0.57

^{a} $\Delta\nu = \nu_0 - \nu_\infty$. ^{b} $\langle\tau_s\rangle = a_1\tau_1 + a_2\tau_2$. ^{c} Error in the measurement is ±5%.

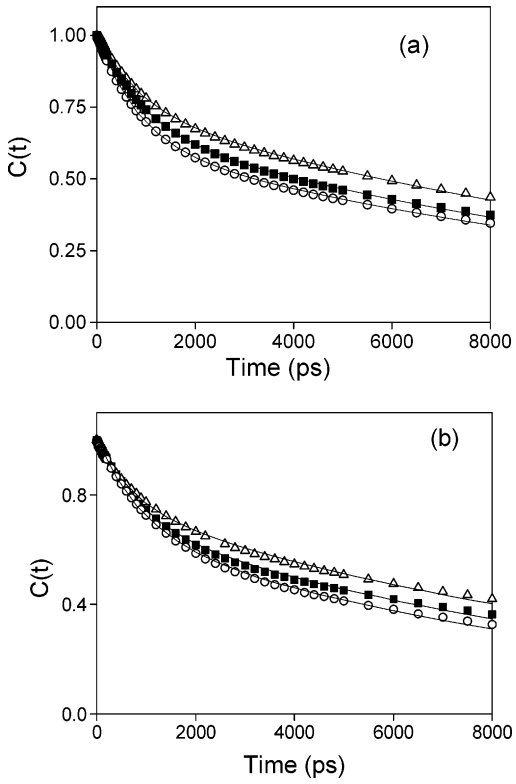

Figure 6. Decay of solvent correlation function ($C(t)$) of C-480 (a) and of C-490 (b) (△) for $w_g = 1.9$, (■) 3, and (○) 3.7.

an initial decay of 55 fs (50%), attributed to the librational motions. Solvent relaxation dynamics of C-480 in water is bimodal with time constants of <50 ps (26%) and 310 fs (74%). The very fast solvent relaxation in water is attributed to the intermolecular vibrational and librational motions. These processes require very small activation energy. The solvation dynamics in other polar solvents such as methanol and acetonitrile are found to take place within the subpicosecond time scale.[13−15,17−19]

The interesting observation is that the solvent relaxation becomes slower on going from pure glycerol to reverse micelles. In pure glycerol, C-490 and C-480 have solvation times of 0.455 and 0.580 ns, respectively. At $w_g = 3.7$ the solvation times for C-490 and C-480 are 7.251 and 8.110 ns, respectively. Similar results were obtained for other reverse micelles also.[29−42]

In pure water and methanol, acetonitrile solvation dynamics occur at the subpicosecond level while in the solvent pool of reverse micelles solvation dynamics is 1000 times retarded.[20−22,29−42] In the present case the interesting observation is that the solvation dynamics in the reverse micellar pool is nearly 10−15 times retarded. However, for water, methanol, and acetonitrile reverse micelles[20−22,29−42] the fast component of solvation dynamics in the reverse micellar pool is not coming from the pure solvent. With picosecond time resolution it is not possible to observe the dynamical Stokes' shift in those solvents. The solvent motion is highly hindered in the nanocage of the glycerol reverse micelles. From Table 4 it is observed that with increasing glycerol content the solvation time decreases. At $w_g = 1.9$ glycerol the solvation times for C-490 and C-480 are 9.70 and 10.50 ns, respectively. These become 7.25 and 8.11 ns at $w_g = 3.7$ for C-490 and C-480, respectively. This phenomenon can be explained by using the dynamic exchange model,[20−22,65] as used by several groups to explain the solvation dynamics in micelles and reverse micelles.[20−24,40−42] In this model,[65] it is assumed that a dynamic exchange occurs between the free and bound solvent molecules. The energetics of the exchange depends on the strength and number of hydrogen bonds among the bound solvent molecules and the biomolecules. As the strength of the hydrogen bond increases, the relative population of the bound solvent molecules increases. Consequently, the relative population of the slow components also increases. This can also explain the existence of solvation dynamics of two different time scales. We can successfully use this model in the case of glycerol reverse micelles to explain the w_g dependency of solvation dynamics. In the case of aqueous reverse micelles Li et al.[66] reported that three or four water molecules might bridge between the sulfonate and sodium ions in the AOT reverse micelles. Basically, the water molecules are strongly bonded to the wall of the reverse micelles through the Na^+ ions. Glycerol can play the same role as water does in aqueous reverse micelles. Glycerol has three hydroxyl groups, which are capable of strong intermolecular bonding. At low w_g values, the glycerol molecules are strongly hydrogen bonded to the wall of the reverse micelles and consequently the system exhibits a longer solvation time at low w_g values. With increasing w_g, glycerol molecules that are bound through hydrogen bonds to the SO_3^- group of AOT increase the number of free glycerol molecules in the core of the reverse micelles, contributing to a faster dynamics at a higher w_g value. Shirota et al.[40] and we[41] observed that for water and methanol reverse micelle solvation dynamics become faster with increasing water and methanol content in the solvent pool while solvation dynamics in acetonitrile reverse micelles are w independent. The lack of hydrogen bonding for acetonitrile was found to be responsible for showing down w independence.

Though ionic dynamics is quite slow and this is verified earlier by various groups,[67−69] in the present study the Na^+ ion may not be playing any role in slowing down the observed dynamics. Huppert et al.[67] observed the slow dynamics in the molten salt and interpreted this as due to translational motion of the ions. Riter et al.[31] studied the effect of counterions in the solvation dynamics of water in AOT reverse micelles. They showed that the dynamics is faster in the presence of NH_4^+ ions compared to Na^+ ions, and this is due to the strong interaction of water with the Na^+ ions present in the interior. Earlier reported slow dynamics in acetonitrile reverse micelles is probably due to the motion of Na^+ ions in solution.[40−41] Recently, Biswas et al.[68] studied the solvation dynamics of nonassociated polar solvents such as acetonitrile by using the molecular hydrodynamic theory (MHT). They also observed that the solvation dynamics in the nonassociated liquids is slow compared to that in water, methanol, and formamide. Because the nonassociated solvents cannot sustain high-frequency librations or vibrations, as there is no hydrogen bonding. Maroncelli et al. reported[69] that unlike the $NaClO_4$/acetonitrile system nanosecond solvation time is not observed in the $NaClO_4$/methanol system. Thus from the above discussion we can conclude that ionic solvation is not important in the present study.

In this context we can compare solvation times as obtained using C-490 and C-480. It is revealed from Table 4 that the solvent relaxation is faster for C-490 compared to that for C-480. We recently reported similar results in Brij micelle[23b] solution where the rotational relaxation time of C-490 is higher than that of C-480 but the solvation time is substancially less. However, in the present case the difference between solvation times for C-480 and C-490 is not statistically different within the given uncertainties. Again the results obtained from the wobbling in a cone model suggest that the two dye molecules

are not situated differently. Therefore it does not merit an interpretation in terms of the positions of the solutes. The little faster slovation in the case of C-490 may be due to deactivation in the excited state by various other processes, e.g., charge-transfer, etc. The other striking observation is that with an increase in glycerol content the fast component increases for C-490 (from 0.740 ns at $w_g = 1.9$ to 0.940 ns at $w_g = 3.7$) while for C-480 the same decreases (0.860 ns at $w_g = 1.9$ to 0.790 ns at $w_g = 3.7$). The possible explanation for this behavior is as follows.

The fast component time in the reverse micellar solvent pool is mainly contributed by the free glycerol molecules and the slow component in solvation time is attributed to the bound solvent molecules. At higher w_g values the number of free glycerol molecules increases. These free glycerol molecules get hydrogen bonded preferably to C-490, as C-490 possesses one $-NH_2$ group. Thus the fast component time of C-490 is retarded with an increase in glycerol. The interaction of glycerol with C-480 is comparatively weaker due to the rigidity of C-480; hence the fast component in the solvation dynamics remains constant. However, an increase in fast component by 200 ps is not significant for the average solvation time in the present case and thus hydrogen bonding of glycerol to solute is not a factor here. The other observation is that solvation times at $w_g = 3.7$ and 3 are closer than the solvation times at $w_g = 1.9$ and 3. This leads us to conclude that on going from $w_g = 3$ to 3.7 the free glycerol does not increase in a significant amount and the environment inside the glycerol solvent pool remains intact. Recently Costa et al.[58] reported that microviscosity remains more or less the same at higher glycerol content.

In the present case though we observed a slow solvent relaxation component, a substantial part of the fast (<90 ps) solvent relaxation component is missed due to the limited time resolution of our setup. We applied the method of Fee and Maroncelli[70] to calculate the missing component in the solvent relaxation dynamics. The time zero spectrum was estimated with this process. The predicted Stokes' shift for C-480 in glycerol reverse micelles is approximately 4203 cm^{-1}, while average value of observed Stokes' shift for the glycerol reverse micellar system is 2000 cm^{-1}. Thus we are missing at least 50% of the total solvent relaxation dynamics. However, with an increase in glycerol content in the reverse micelles the missing component also increases. In the case of C-490 the predicted Stokes' shift in glycerol reverse micelles is approximately 2200 cm^{-1} and the average value of observed Stokes' shift for the glycerol reverse micellar system is 1100 cm^{-1}. Thus in this case also we missed at least 50% of the total solvation dynamics. Here also we observed that the missing component increases with an increase in the glycerol content inside the reverse micellar pool.

In this context it would be interesting to make a comparison between the solvation dynamics in glycerol containing reverse micelles and in other low viscous polar solvents such as water, methanol, and acetonitrile reverse micelles.[29−42] While solvation dynamics is several thousand times slower in water, methanol, and acetonitrile reverse micelles[29−42] the than that in pure solvents, in the case of glycerol reverse miclles solvation dynamics is 20 times slower than that in pure glycerol. The interesting observation is that in IL confined reverse micelles[54a] the retardation in solvation dynamics was observed to be 2−3 times that in pure IL although the present system does not have any resemblance to IL confined reverse micelles except IL has much higher viscosity compared to conventional polar solvents such as water, methanol, etc. Thus slowing down in solvation time by 2−20 times in IL and glycerol reverse micelles compared to pure IL and glycerol and several thousand times slowing down in water, methanol, or acetonitrile reverse micelles compared to pure water, methanol, and acetonitrile indicates that retardation of solvation time of polar solvents in a reverse micelles is not only guided by hydrogen bonded dynamics but is also very much depended on the viscosity of the solvent. In the case of more viscous solvents, e.g., glycerol or IL, the retardation in solvation time is much smaller compared to that of pure solvents such as water or methanol. So the viscosity of the polar solvents is very important in determining the dynamics in the confined cavity of reverse micelles. This may be verified by a comparison between experimental and computer simulation studies.

4. Conclusion

This work reveals that solvation dynamics of glycerol becomes slower in the nanocavity of the reverse micelles compared to that in pure glycerol solution. However, the slowing down of solvation dynamics in glyerol reverse micelles is not comparable to that in water reverse micelles. We observed only a 20 to 30 times retardation of solvation dynamics in glycerol reverse micelles compared to the pure solvent while in water, methanol, and acetonitrile reverse micelles the retardation of solvation dynamics is several thousand times compared to that in pure solvent. While solvation dynamics is found to be retarded, the rotational relaxation time is found to increase with addition of glycerol content. This is supposed to be arising from the strong hydrogen bonding between glycerol and solute molecules and due to the increase in the microviscosity inside the reverse micellar pool.

Acknowledgment. N.S. is thankful to the Department of Science and Technology (DST), Government of India for a generous research grant. A.C., D.S., and P.S. are thankful to CSIR for research fellowships. The authors also thank Basudeb Haldar, Arabinda Mallick, and Prof. Nitin Chattopadhyay of Jadavpur University for allowing us to use the spectrofluorimeter and an anonymous reviewer for constructive comments and suggestions.

References and Notes

(1) (a) *Structure and Reactivity in Reverse Micelles*; Pileni, M. P., Ed.; Studies in Physical and Theoretical Chemistry, Vol. 65; Elsevier: Amsterdam, The Netherlands, 1989. (b) Luisi, P. L.; Straube, B. E., Eds. *Reverse Micelles*; Plenum Press: NewYork, 1984. (c) Luisi, P. L. *Adv. Chem. Phys.* **1996**, *92*, 425. (d) Pileni, M. P. *J. Phys. Chem.* **1993**, *97*, 6961.

(2) Kitahara, A. *Adv. Colloid Interface Sci.* **1980**, *12*, 109.

(3) Moulik, S. P.; Paul, B. K. *Adv. Colloid Interface Sci.* **1998**, *78*, 99.

(4) de Gennes, P. G. *Rev. Mod. Phys.* **1992**, *64*, 645.

(5) Cho, C. H.; Singh, S.; Robinson, G. W. *Faraday Discuss.* **1996**, *103*, 1.

(6) De, T. K.; Maitra, A. *Adv. Colloid Interface Sci.* **1995**, *59*, 95.

(7) Langevin, D. *Acc. Chem. Res.* **1988**, *21*, 255.

(8) Riter, R. E.; Kimmel, J. R.; Undiks, E. P.; Levinger, N. E. *J. Phys. Chem. B* **1997**, *101*, 8292.

(9) (a) Raju, B. B.; Costa, S. M. B. *J. Phys. Chem. B* **1999**, *103*, 4309. (b) Costa, S. M. B. *Phys. Chem. Chem. Phys.* **1999**, *1*, *5029.* (c) Seth, D.; Chakrabarty, D.; Chakraborty, A.; Sarkar, N. *Chem. Phys. Lett.* **2005**, *401*, 546. (d) Borsarelli, C. D.; Cosa, J. J.; Previtali, C. M. *Langmuir* **1992**, *8*, 1070. (e) Sato, C.; Kikuchi, K. *J. Phys. Chem.* **1992**, *96*, 5601.

(10) Jimenez, R.; Fleming, G. R.; Kumar, P. V.; Maroncelli, M. *Nature* **1994**, *369*, 471.

(11) Lang, M. J.; Jordanides, X. J.; Song, X.; Fleming, G. R. *J. Chem. Phys.* **1999**, *110*, 5884.

(12) Vajda, S.; Jimenez, R.; Rosenthal, S. J.; Fidler, V.; Fleming, G. R.; Castner, E. W., Jr. *J. Chem. Soc., Faraday Trans.* **1994**, *91*, 867.

(13) Kahlow, M. A.; Kang, T. J.; Barbara, P. F. *J. Chem. Phys.* **1988**, *88*, 2372.

(14) Jarzeba, W.; Barbara, P. F. *Adv. Photochem.* **1990**, *15*, 1.
(15) Kahlow, M. A.; Jarzeba, W.; Kang, T. J.; Barbara, P. F. *J. Chem. Phys*. **1989**, *90*, 151.
(16) Fee, R. S.; Milsom, J. A.; Maroncelli, M. *J. Phys. Chem.* **1991**, *95*, 5170.
(17) Maroncelli, M. *J. Mol. Liq*. **1993**, *57*, 1.
(18) Horng, M. L.; Gardecki, J. A.; Papazyan, A.; Maroncelli, M. *J. Phys. Chem*. **1995**, *99*, 17311.
(19) Glasbeek, M.; Zhang, H. *Chem. Rev.* **2004**, *104*, 1929.
(20) Bhattacharyya, K. *Acc. Chem. Res.* **2003**, *36*, 95.
(21) Bhattacharyya, K.; Bagchi, B. *J. Phys. Chem. A* **2000**, *104*, 10603.
(22) Nandi, N.; Bhattacharyya, K.; Bagchi, B. *Chem. Rev*. **2000**, *100*, 2013.
(23) (a) Sarkar, N.; Datta, A.; Das, S.; Bhattacharyya, K. *J. Phys. Chem.* **1996**, *100*, 15483. (b) Chakrabarty, D.; Hazra, P.; Chakraborty, A.; Sarkar, N. *Chem. Phys. Lett*. **2003**, *392*, 340. (c) Tamoto, Y.; Segawa, H.; Shirota, H. *Langmuir* **2005**, *21*, 3757.
(24) (a) Chakrabarty, D.; Hazra, P.; Sarkar, N. *J. Phys. Chem. A* **2003**, *107*, 5887. (b) Chakrabarty, D.; Hazra, P.; Chakraborty, A.; Sarkar, N. *J. Phys. Chem. B* **2003**, *107*, 13643. (c) Chakrabarty, D.; Chakraborty, A.; Seth, D.; Hazra, P.; Sarkar, N. *J. Chem. Phys.* **2005**, *122*, 184516.
(25) Frauchiger, L.; Shirota, H.; Uhrich, K. E.; Castner, E. W., Jr. *J. Phys. Chem. B* **2002**, *106*, 7463.
(26) (a) Hof, M. Solvent Relaxation in Biomembranes. In. *Applied Fluorescence in Chemistry, Biology and Medicine*; Rettig, W., Ed.; Springer-Verlag: Berlin, Germany, 1999; p 439. (b) Hutterer, R.; Schneider, F. W.; Sprinz, H.; Hof, M. *Biophys. Chem.* **1996**, *61*, 151.
(27) Pal, S. K.; Zewail, A. H. *Chem. Rev.* **2004**, *104*, 2099.
(28) Pal, S. K.; Peon, G.; Bagchi, B.; Zewail, A. H. *J. Phys. Chem. B* **2002**, *106*, 12376.
(29) Sarkar, N.; Das, K.; Datta, A.; Das, S.; Bhattacharyya, K. *J. Phys. Chem.* **1996**, *100*, 10523.
(30) Das, S.; Datta, A.; Bhattacharyya, K. *J. Phys. Chem. A* **1997**, *101*, 3299.
(31) Riter, R. E.; Willard, D. M.; Levinger, N. E. *J. Phys. Chem. B* **1998**, *102*, 2705.
(32) Pant, D.; Riter, R. E.; Levinger, N. E. *J. Chem. Phys.* **1998**, *109*, 9995.
(33) Riter, R. E.; Undiks, E. P.; Levinger, N. E. *J. Am. Chem. Soc*. **1998**, *120*, 6062.
(34) Willard, D. M.; Riter, R. E.; Levinger, N. E. *J. Am. Chem. Soc*. **1998**, *120*, 4151.
(35) Willard, D. M.; Levinger, N. E. *J. Phys. Chem. B* **2000**, *104*, 11075.
(36) Riter, R. E.; Kimmel, J. R.; Undiks, E. P.; Levinger, N. E. *J. Phys. Chem. B* **1997**, *101*, 8292.
(37) Levinger, N. E. *Curr. Opin. Colloid Interface Sci.* **2000**, *5*, 118.
(38) Lundgren, J. S.; Heitz, M. P.; Bright, F. V. *Anal. Chem*. **1995**, *67*, 3775.
(39) Riter, R. E.; Undiks, E. P.; Kimmel, J. R.; Levinger, N. E. *J. Phys. Chem. B* **1998**, *102*, 7931.
(40) Shirota, H.; Horie, K. *J. Phys. Chem. B* **1999**, *103*, 1437.
(41) (a) Hazra, P.; Sarkar, N. *Chem. Phys. Lett.* **2001**, *342*, 303. (b) Hazra, P.; Sarkar, N. *Phys. Chem. Chem. Phys.* **2002**, *4*, 1040. (c) Hazra, P.; Chakrabarty, D.; Sarkar, N. *Chem. Phys. Lett*. **2002**, *358*, 523. (d) Hazra, P.; Chakrabarty, D.; Sarkar, N. *Langmuir* **2002**, *18*, 7872. (e) Hazra, P.; Chakrabarty, D.; Sarkar, N. *Chem. Phys. Lett.* **2003**, *371*, 553. (f) Hazra, P.; Chakrabarty, D.; Sarkar, N. *Langmuir* **2002**, *18*, 7872.
(42) Shirota, H.; Segawa, H. *Langmuir* **2004**, *20*, 329.
(43) (a) Pal, S.; Bagchi, B.; Balasubramanium, S. *J. Phys. Chem. B* **2005**, *109*, 12879. (b) Balasubramanian, S.; Pal, S.; Bagchi, B. *Phys. Rev. Lett.* **2002**, *89*, 115505. (c) Pal, S.; Balasubramanian, S.; Bagchi, B. *J. Phys. Chem. B* **2003**, *107*, 5194.
(44) (a) Faeder, J.; Ladanyi, B. M. *J. Phys. Chem. B* **2005**, *109*, 6732. (b) Faeder, J.; Ladanyi, B. M. *J. Phys. Chem. B* **2001**, *105*, 11148.
(45) (a) Thompson, W. H. *J. Chem. Phys.* **2004**, *120*, 8125. (b) Thompson, W. H. *J. Chem. Phys.* **2002**, *117*, 6618.
(46) (a) Senapati, S.; Berkowitz, M. L. *J. Phys. Chem. A* **2004**, *108*, 9768. (b) Senapati, S.; Keiper, J. S.; DeSimone, J. M.; Wignall, G. D.; Melnichenko, Y. B.; Frielinghaus, H.; Berkowitz, M. L. *Langmuir* **2002**, *18*, 7371.
(47) Senapati, S.; Chandra, A. *J. Phys. Chem. B* **2001**, *105*, 5106.
(48) (a) Sando, G. M.; Dahl, K.; Owrutsky, J. C. *J. Phys. Chem. A* **2004**, *108*, 11209. (b) Sando, G. M.; Dahl, K.; Zhong, Q.; Owrutsky, J. C. *J. Phys. Chem. A* **2005**, *109*, 5788.
(49) Kelkar, D. A.; Chattopadhyay, A. J. *Phys. Chem. B* **2004**, *108*, 12151.
(50) (a) Karmakar, R.; Samanta, A. *J. Phys. Chem. A* **2002**, *106*, 4447. (b) Karmakar, R.; Samanta, A. *J. Phys. Chem. A* **2002**, *106*, 6670. (c) Karmakar, R.; Samanta, A. *J. Phys. Chem. A* **2003**, *107*, 7340. (d) Saha, S.; Mandal, P. K.; Samanta, A. *Phys. Chem. Chem. Phys.* **2004**, *6*, 3106.
(51) (a) Ingram, J. A.; Moog, R. S.; Ito, N.; Biswas, R.; Maroncelli, M. *J. Phys. Chem. B* **2003**, *107*, 5926. (b) Ito, N.; Arzhantsev, S.; Heitz, M.; Maroncelli, M. *J. Phys. Chem. B* **2004**, *108*, 5771. (c) Arzhantsev, S.; Ito, N.; Heitz, M.; Maroncelli, M. *Chem. Phys. Lett.* **2003**, *381*, 278. (d) Ito, N.; Arzhantsev, S.; Maroncelli, M. *Chem. Phys. Lett.* **2004**, *396*, 83.
(52) (a) Chakrabarty, D.; Hazra, P.; Chakraborty, A.; Seth, D.; Sarkar, N. *Chem. Phys. Lett.* **2003**, *381*, 697. (b) Chakrabarty, D.; Chakraborty, A.; Seth, D.; Sarkar, N. *J. Phys. Chem. A* **2005**, *109*, 1764.
(53) (a) Anderson, J. L.; Pino, V.; Hagberg, E. C.; Sheares, V. V.; Armstrong, D. W. *Chem. Commun.* **2003**, 2444. (b) Fletcher, K. A.; Pandey, S. *Langmuir* **2004**, *20*, 33.
(54) (a) Chakrabarty, D.; Seth, D.; Chakraborty, A.; Sarkar, N. *J. Phys. Chem. B* **2005**, *109*, 5753. (b) Chakraborty, A.; Seth, D.; Chakrabarty, D.; Setua, P.; Sarkar, N. *J. Phys. Chem. A* **2005**, *109*, 11110.
(55) Gao, H.; Li, J.; Han, B.; Chen, W.; Zhang, J.; Zhang, R.; Yan, D. *Phys. Chem. Chem. Phys.* **2004**, *6*, 2914.
(56) (a) Laia, C. A. T.; Cornejo, P. L.; Costa, S. M. B.; d'Oliveira, J.; Martinho, J. M. G. *Langmuir* **1998**, *14*, 3531. (b) Laia, C. A. T.; Brown, W.; Almgren, M.; Costa, S. M. B. *Langmuir* **2000**, *16*, 8763.
(57) Chakraborty, A.; Seth, D.; Chakrabarty, D.; Hazra, P.; Sarkar, N. *Chem. Phys. Lett.* **2005**, *405*, 18.
(58) Laila, C. A. T.; Costa, S. M. B. *Langmuir* **2002**, *18*, 1494.
(59) (a) Dutt, G. B.; Ghanty, T. K. *J. Phys. Chem. A* **2004**, *108*, 6090. (b) Dutt, G. B.; Ghanty, T. K. *J. Chem. Phys.* **2003**, *119*, 4768.
(60) Kim, T. G.; Topp, M. R. *J. Phys. Chem. A* **2004**, *108*, 7653.
(61) Quitevis, F. L.; Marcus, A. H.; Fayer, M. D. *J. Phys. Chem.* **1993**, *97*, 5762.
(62) Maiti, N. C.; Krishna, M. M. G.; Britto, P. J.; Periasamy, N. *J. Phys. Chem. B* **1997**, *101*, 11051.
(63) Dutt, G. B. *J. Phys. Chem. B* **2003**, *107* 10546.
(64) Maroncelli, M.; Fleming, G. R. *J. Chem. Phys.* **1987**, *86*, 6221.
(65) (a) Nandi, N.; Bagchi, B. *J. Phys. Chem. B* **1997**, *101*, 10954. (b) Nandi, N.; Bagchi, B. *J. Phys. Chem. A* **1998**, *102*, 8217.
(66) Li, Q.; Weng, S.; Wu, J.; Zhou, N. *J. Phys. Chem. B* **1998**, *102*, 3168.
(67) (a) Bart, E.; Huppert, D. *Chem. Phys. Lett.* **1992**, *195*, 37. (b) Bart, E.; Meltsin, A.; Huppert, D. *J. Phys. Chem.* **1994**, *98*, 3295. (c) Bart, E.; Meltsin, A.; Huppert, D. *J. Phys. Chem.* **1994**, *98*, 10819.
(68) Biswas, R.; Bagchi, B. *J. Phys. Chem. A* **1999**, *103*, 2495.
(69) Chapman, C. F.; Maroncelli, M. *J. Phys. Chem*. **1991**, *95*, 9095.
(70) Fee, R. S.; Maroncelli, M. *Chem. Phys.* **1994**, *183*, 235.